technical transactions

No. 2025/019

civil engineering and transport

sciendo

Numerical prediction of shallow footing settlements using HS-Brick model calibrated from laboratory and in situ tests

Andrzej Truty
andrzej.truty@pk.edu.pl | https://orcid.org/0000-0002-2248-9236
Cracow University of Technology, Poland
Rafał Obrzud
rafal.obrzud@kfsa.ch | https://orcid.org/0009-0005-9608-6076
Karakas & Français, Switzerland

Scientific Editor: Andrzej Winnicki, Cracow University of Technology
Technical Editor: Aleksandra Urzędowska, Cracow University of Technology Press
Typesetting: Małgorzata Murat-Drożyńska, Cracow University of Technology Press

Received: October 23, 2025
Accepted: December 1, 2025

Data Availability Statement: All relevant data are within the paper and its Supporting Information files.

Competing interests: The authors have declared that no competing interests exist.

Citation: Truty, A., Obrzud, R. (2025). Numerical prediction of shallow footing settlements using HS-Brick model calibrated from laboratory and in situ tests. Technical Transactions, e2025019. https://doi.org/10.37705/TechTrans/e2025019

Abstract

This study presents a robust methodology for calibrating the Hardening Soil–Brick (HS-Brick) constitutive model using both laboratory and field tests. Model parameters are derived and verified against a benchmark problem involving a spread footing founded on overconsolidated sandy soil in Texas, based on large-scale experiments by Briaud and Gibbens. The results show that wide variations in confining stress complicate direct parameter estimation from triaxial tests, necessitating the use of global optimization methods. To reduce computational cost, a metamodeling approach based on Latin hypercube sampling is employed, enabling efficient surrogate predictions that serve as the computational engine for evolutionary algorithms. The proposed framework provides accurate and computationally efficient settlement predictions and is readily adaptable for reliability-based geotechnical design applications.

Keywords: Hardening Soil-Brick model, CPTU/CHT tests, FEM simulations, Shallow foundations, Parameters calibration

1. Introduction

The analysis of serviceability limit states remains one of the most demanding tasks in contemporary geotechnical engineering. This challenge is particularly critical in the design of deep excavations and complex piled-raft foundations, which cannot be adequately assessed using simplified analytical methods. Reliable prediction of deformations and internal forces within the underground parts of a structure requires the application of numerical approaches—most commonly those based on the Finite Element Method (FEM)—in conjunction with advanced constitutive soil models which are capable to represent soil behavior from very small to moderate strain amplitudes.

The Hardening Soil–Brick (HS-Brick) model (Cudny & Truty, 2020), which is a significantly improved version of the previous Hardening Soil–Small (HSs) one originally proposed by Benz (Benz, 2007; Niemunis & Cudny, 2018; Schanz & Vermeer, 1998; Schanz et al.,1999), is one of the most advanced constitutive formulations currently available in commercial use and has been widely adopted in the engineering practice over the last two decades. The HS-Brick model uses the same set of parameters as its predecessor, except for several enhanced features with respect to stiffness barotropy. In the original formulation, all the stiffness moduli depend on the minor principal effective stress (σ_3), whereas in the HS-Brick model the power law can also be expressed as a function of the mean effective stress (p'). In general, the latter approach provides better predictive performance, as it more accurately captures the stress-dependency of soil stiffness in natural conditions.

An additional improvement introduced in the HS-Brick model addresses the prediction of undrained shear strength. It is well known that the earlier model tended to produce unrealistically high, even unbounded, undrained shear strength values when the dilatancy angle was nonzero. In order to avoid this drawback, a refined formulation was proposed by Truty and Obrzud (2015), ensuring a more realistic representation of undrained behavior.

As the advanced laboratory tests may turn out time-consuming and expensive, the calibration of geotechnical characteristics, and specifically Hardening Soil parameters may rely on in-situ soundings such as CPTU and SDMT. These tests should be completed by a sufficient number of laboratory tests (triaxial and oedometer) to enable tunning or validating empirical correlations for essential parameters. In the case of heavily compacted deposits, where the piezocone soundings (CPTU) or Marchetti dilatometer tests (DMT) cannot be carried out, other tests which relies on borehole-based test such as cross-hole test (CHT), standard penetration test (SPT), or Menard pressuremeter test (PMT) have to be used. The comprehensive studies by Wichtmann (Wichtmann et al, 2017; Wichtmann & Triantafyllidis, 2009) provided one of the key foundations for Truty (Truty, 2024), who showed that, based on CPTU predictions, almost all reference stiffness moduli—E_0^{ref}, $E_{\text{ur}}^{\text{ref}}$, E_{50}^{ref}, $E_{\text{oed}}^{\text{ref}}$ and —as well as the stiffness exponent m, can be calibrated with an estimated error of about ±20%.. Ongoing research aims to extend this methodology to cohesive soils. A similar trend is observed in recent publications, where constitutive models are calibrated using in-situ test data (Lai et al., 2025) which may offer significant potential for the application for stochastic methods (Kawa et al, 2025; Kawa et al., 2025). A comprehensive study of certain calibration methodologies and selected benchmarks are analyzed in report (Obrzud & Truty, 2020).

In the present study, the variability of HS-Brick model parameters derived from triaxial, CPTU, DMT, and CHT tests is examined. Based on the obtained experimental data, a complete set of initial model parameters is established and subsequently verified against a benchmark problem involving a spread footing founded on silty sands at A&M University's National Geotechnical Site in Texas. Although such a problem can be analyzed using various analytical approaches, the findings of Briaud and Gibbens (Briaud & Gibbens, 1997; Briaud & Gibbens, 1999) clearly indicate that simplified methods may produce important

https://doi.org/10.37705/TechTrans/e2025019

discrepancies between predicted and measured settlements.

The main objective of this paper is to present an efficient calibration methodology based on both laboratory and field test data, and to evaluate the accuracy of the resulting settlement predictions. Since field and laboratory tests provide complementary information, special attention is given to the measurement of shear wave velocity both in situ and under corresponding laboratory stress conditions. This paper is organized as follows. Section 2 describes the experiment setup. Section 3 presents the calibration of model parameters based on the results of triaxial, CPTU, DMT, SPT, and CHT field tests, and concludes with a summary of the identified parameters. Section 4 describes the numerical FEM model, including the initial and boundary conditions, loading program, and results of the sensitivity analysis. Finally, the main conclusions are drawn in Section 5.

2. Experiment setup

To assess the ability of the HS-Brick model to predict the settlements of spread footings, the *South Footing* (3 m × 3 m) reported in (Briaud & Gibbens, 1997; Briaud & Gibbens, 1999) was examined. The tests which are closely located to the footing are considered in the present study: DMT-1, DMT-2, SPT-1 and CHT-1. It is not clearly indicated in (Briaud & Gibbens, 1997) what was the height of the overburden removed prior to the installation of the footings. The height of 1.5 m was deduced. The site stratigraphy is presented in Fig.1.

After removal of the 1.5 m overburden, the subsoil profile consists of a 3.5 m thick layer of medium-dense silty fine sand (layer I), underlain by a 3.5 m layer of medium-dense silty sand containing clay and gravel (layer II), and a 4.0 m layer of medium-dense silty sand to sandy clay with gravel (layer III). These sand layers overlie a very hard, dark gray clay layer, which is assumed to be infinitely stiff for modeling purposes. The phreatic water surface is located at a depth of 4.9 m, and the footing is embedded 0.889 m into the subsoil.

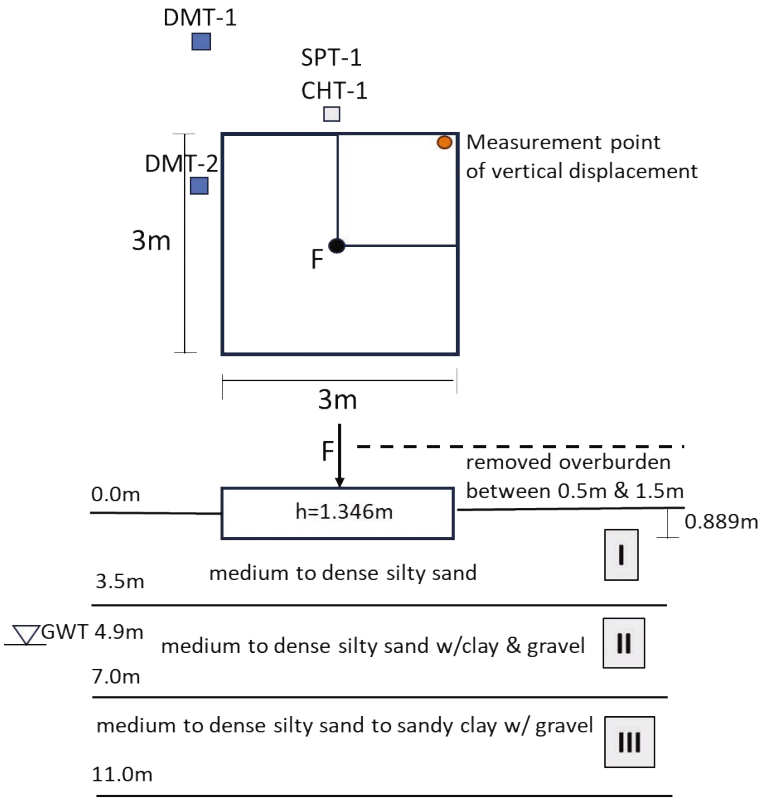

Fig. 1. Draft of the test setup (south footing nr 3) and soil stratigraphy at A&M University's National Geotechnical Site in Texas (Briaud & Gibbens, 1997) (own elaboration)

3. Determination of HS-Brick model parameters from laboratory and field tests results

To perform the numerical analysis predicting the load–settlement response of the square footing under a complex loading program, the HS-Brick model parameters were derived from an extensive experimental database published in (Briaud & Gibbens, 1997). This database includes two isotropically-consolidated drained (CD) triaxial tests on remolded soil samples, one CPTU test (CPT-7), two DMT tests (DMT-1 and DMT-2), one cross-hole test (CHT-1), and one standard penetration test (SPT-1). In the present study, particular attention is given on the laboratory testing, CPTU, and cross-hole test results, which are discussed in the following subsections.

3.1. Triaxial tests

Two drained triaxial tests were performed on remolded soil samples collected at two depths, 0.6 m (Layer I) and 3.0 m (Layer II), respectively. These tests were carried out without unloading–reloading cycles; therefore, their interpretative value is somewhat limited. Firstly, the microstructure of the remolded specimens does not represent the in-situ soil fabric, and each sample may exhibit a different initial overconsolidation ratio (OCR). A qualitative analysis of the triaxial test results at both depths indicates that, under low confining pressures, the samples behave as highly overconsolidated, whereas under the highest confining pressure (345 kPa), the soil response corresponds to normally consolidated behavior. This conclusion is further supported by the ε_v–ε_1 relationship, where for σ_3 = 345 kPa, dilatancy is no longer observed. Consequently, four HS-Brick model parameters can be considered as particularly significant i.e. the secant reference stiffness modulus E_{50}^{ref} the stress-dependency exponent m, the initial preconsolidation pressure p_{co} and the dilatancy parameter D appearing in the modified Rowe's dilatancy law which governs soil compressibility within the contractant domain. The unloading–reloading modulus $E_{\text{ur}}^{\text{ref}}$ as well as the tangent oedometric modulus $E_{\text{oed}}^{\text{ref}}$ are assumed to be correlated with the secant E_{50}^{ref} modulus according to the empirical relationships proposed for sandy soils (Truty, 2024):

$$\frac{E_{\text{ur}}^{\text{ref}}}{E_{50}^{\text{ref}}} = 2 + 6.93 \exp\left(-0.10107 \frac{E_{50}^{\text{ref}}}{p_a} \right) \tag{1}$$

$$\frac{E_{\text{oed}}\left(\sigma_v = 8 p_a\right)}{E_{50}^{\text{ref}}} = 69.7 \left(\frac{E_{50}^{\text{ref}}}{p_a} \right)^{-0.489} \tag{2}$$

where σ_v is the reference vertical stress value at which the tangent oedometer modulus on the virgin consolidation line is defined, and p_a is the reference stress corresponding to the atmospheric pressure (p_a = 100 kPa).

The remaining model parameters were fixed and assumed as: ϕ' = 36.25°, c = 3.5 kPa, ν = 0.15, R_f = 0.95 and ψ = 1.9° for sample collected at depth 0.6m and ϕ' = 34.4°, c = 5 kPa, ν = 0.2, and ψ = 1.9° for the one collected at depth 3m, respectively. As the formula (2), which was designed for fine sands with a high fines content, is based on a very limited database and may generate values that cannot be reproduced by the model, an additional study has indicated that the optimal ratio between these two moduli at a reference stress of $\sigma_v = p_a$ can be assumed as $E_{\text{oed}}(\sigma_v = p_a) = 1.2\, E_{50}^{\text{ref}}$

The standard HS-Brick model, as well as its predecessor (HSsmall), are unable to accurately reproduce the dilatant behavior of granular soils under varying confining pressures. This limitation is typically manifested by the ε_v–ε_1 curves becoming nearly parallel at larger strains, which is inconsistent

https://doi.org/10.37705/TechTrans/e2025019

with experimental observations. However, the refinement proposed in (Truty & Obrzud, 2015) can reproduce the actual soil response with a higher degree of accuracy. Hence, this model extension is adopted in the present study. Determining the optimal values of the four model parameters constitutes a classical inverse problem, which in most cases cannot be efficiently solved using simple gradient-based optimization methods. Instead, the global optimization algorithms such as Particle Swarm Optimization (PSO) or Differential Evolution (DE) are more appropriate. Since these algorithms require a large number of evaluations of the objective function, it becomes evident that direct finite element (FEM) simulations of the three triaxial tests must be replaced by computationally efficient surrogate models, so called metamodels. In this study, Kriging metamodels were developed to approximate several response quantities. Specifically, metamodels were developed for each of the soil samples for the deviatoric stress (q) at three strain levels (ε_1 = 0.5%, 1.0%, and 1.5%), for the peak volumetric strain ($\varepsilon_{v,\,peak}$), and for the volumetric strain ε_v at = $\varepsilon_1 = 15\%$. Each of these metamodels was generated using 200 parameter samples. The sampling was based on the following probabilistic assumptions: a lognormal distribution for the stress-dependency exponent m (mean value 0.6, standard deviation ≈ 0.05, bounds 0.5–0.7); a uniform distribution for the reference stiffness modulus E_{50}^{ref} (bounds 12–16MPa); a uniform distribution for the dilatancy parameter *D* (bounds 0–0.6); and a uniform distribution for the initial preconsolidation pressure p_{co} (bounds 100–600 kPa).

A sample set of 200 was sufficient to achieve metamodel maximum leave-one-out (LOO) error below 0.1%, indicating very high modelling accuracy. Based on the developed metamodels, a sensitivity analysis using Kucherenko indices was performed, confirming the appropriate selection of key parameters. Due to the limited scope of this study, detailed results of the sensitivity analysis are not presented. However, the general conclusion is that the shear characteristics $(q-\varepsilon_1)$ are primarily influenced by two parameters E_{50}^{ref}, and m, while the dilation characteristics $(\varepsilon_v-\varepsilon_1)$ are affected by all four parameters, with the magnitude of influence varying depending on whether the sample is highly, normally, or lightly overconsolidated.

The optimal parameters set obtained using the DE algorithm, with the generated metamodels serving as the objective function engines, yielded good model response, as shown in Fig. 2 and Fig. 3. For the triaxial test conducted on samples collected at depth 0.6m the optimal parameters have been identified $m = 0.67$, $E_{50}^{\text{ref}} = 12034$ kPa, $D = 0.3$, $p_{co} = 540$ kPa. The same derived parameters, excluding the friction angle, were then used to simulate triaxial test for samples collected at depth 3m.

It should be noted that the obtained optimal parameter values are indicative and not intended to represent in situ soil behavior.

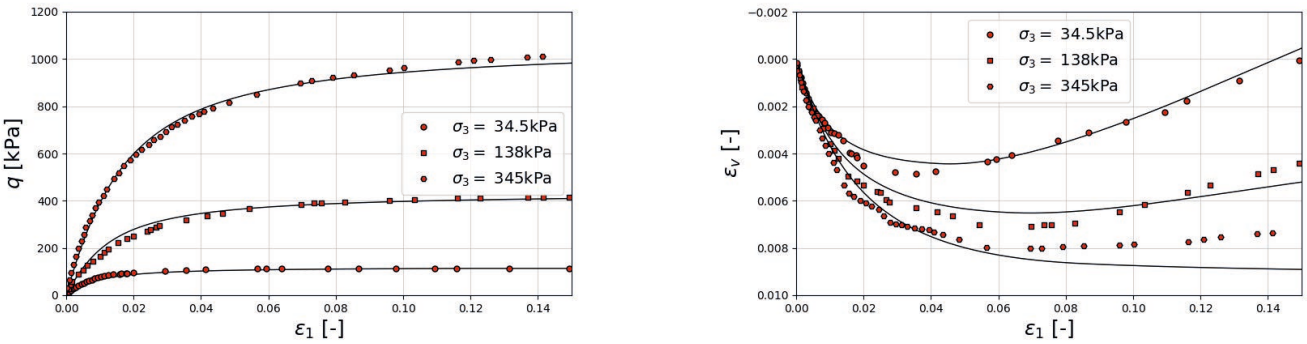

Fig. 2. Comparison of predicted and experimental shear and dilatancy characteristics for sampling depth 0.6m (own elaboration)

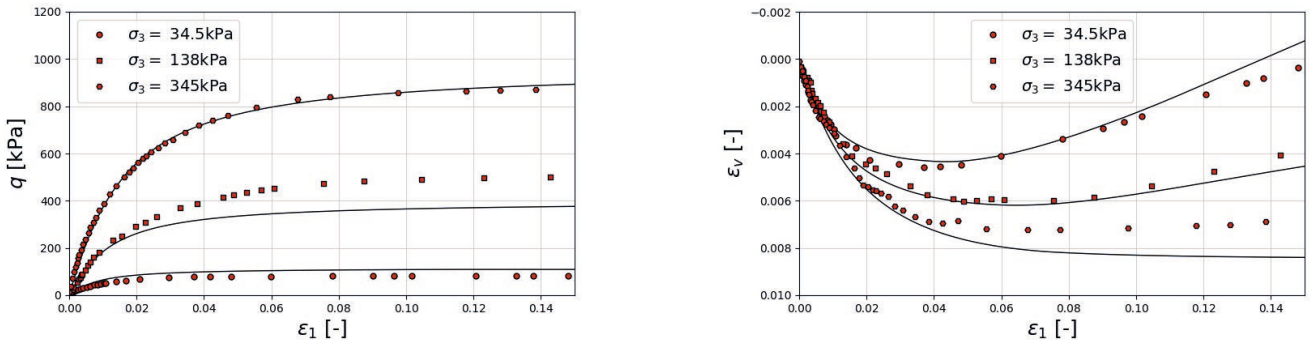

Fig. 3. Comparison of predicted and experimental shear and dilatancy characteristics for sampling depth 3m (own elaboration).

3.2. CPTU and Crosshole tests

In this section, the CPTu test (CPT-7) and cross-hole tests (CHT-1, CHT-2) are interpreted to derive reference stiffness moduli for all geotechnical layers represented by the HS-Brick model. The inclusion of the cross-hole test is essential to avoid significant prediction errors, as the measured piezocone resistances range from 6 to 10 MPa, which is relatively low for sandy soils. Consequently, standard correlation formulas proposed by Robertson (Robertson & Cabal, 2022), Andrus (Andrus et al., 2007), and Truty (Truty et al., 2024) for non-aged sands yield comparatively low initial stiffness moduli (see Fig. 4), which are inconsistent with the cross-hole test results. This discrepancy likely reflects the influence of aging or preconsolidation effects, which are not readily detectable in sandy soils. Inherent anisotropy can be another source of discrepancies. It should be noted that the shear-wave velocity profiles obtained from the two cross-hole tests conducted in orthogonal directions exhibit considerable discrepancies, particularly within the upper 6 meters of the soil profile. Consequently, the averaged shear-wave velocity values were adopted for subsequent analyses.

The shear wave velocity profiles from the crosshole tests indicate that, in geotechnical layers I and II, the aging/preconsolidation indicator K_G^* exceeds the typical threshold ($K_G^* = 330$), suggesting that preconsolidation effects should be considered in these layers (see Fig.5). Notably, the observed discrepancy occurs below the assumed position of the water table. Therefore, the calibration of stiffness moduli must be approached with care: the initial moduli E_0^{ref} are

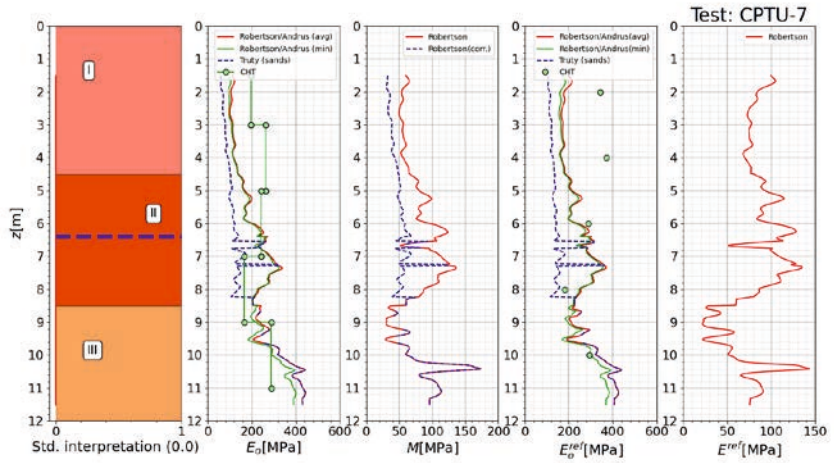

Fig. 4. Comparison of stiffness moduli obtained from standard correlation formulas for sands and from cross-hole test measurements, illustrating the significant underestimation of initial stiffness by the correlation formulas relative to in-situ values (own elaboration)

https://doi.org/10.37705/TechTrans/e2025019

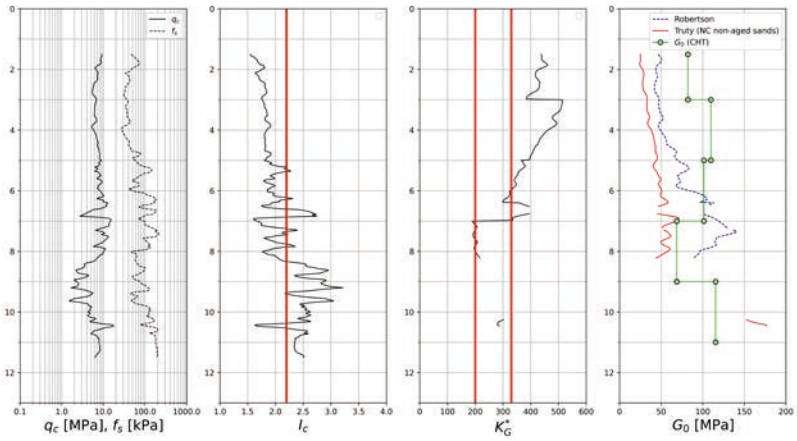

Fig. 5. Analysis of the aging/preconsolidation indicator K_G^* in sandy geotechnical layers, highlighting layers where preconsolidation effects are significant (own elaboration)

expected to be high, while the unloading-reloading moduli E_{ur}^{ref} and the secant moduli E_{50}^{ref} should be adjusted according to the correlation with derived E_0^{ref} directly from the CPTu data.

The power exponent which in the HS-Brick model must be the common for all moduli, can be estimated from the soil behavior type index I_c using the formula (Truty, 2024)

$$m = 0.322 + 0.111\, I_c \tag{3}$$

For layers I and II, where I_c ranges between 1.8 and 2.0, the average power exponent is $m = 0.53$.

To simplify the analysis, it is assumed that the non-aged initial reference stiffness modulus E_0^{ref} is common for both layers I and II and is likely close to the value estimated using Truty's (Truty, 2024) empirical formula (see Fig.4). It should be noted that this formula has an estimated error margin of ±18% (Truty, 2024), implying that E_0^{ref} may vary from 100 to 140 MPa. Consequently, the corresponding reference secant modulus E_{50}^{ref} could range from approximately 13 to 35 MPa, representing a substantial variation.

In practice, all geotechnical parameters should be estimated in a conservative manner. Therefore, as an initial approximation, E_0^{ref} = 100MPa (about 90% of the interpreted value) is adopted for layers I and II.

To illustrate this procedure, the calibration of stiffness moduli for layer I is analyzed. Based on the crosshole test results, the average modulus is approximately 360 MPa. The next step is to estimate , which can be derived from using the empirical formula proposed by Truty for non-aged fine sands with a nonzero fines content:

$$\frac{G_0^{ref}}{E_{50}^{ref}} = 1 + 721.2\left(\frac{E_{50}^{ref}}{p_a}\right)^{-1.19} \tag{4}$$

Substituting $E_0^{ref} \approx 100\,\text{MPa}$ (see Fig. 4) into Equation (4) yields $E_{50}^{ref} \approx 19.3\,\text{MPa}$. Applying Equation (1) subsequently gives $E_{ur}^{ref} \approx 55.56\,\text{MPa}$.

For layer III, the relationships developed by Truty (Truty, 2024) are not directly applicable. Therefore, a simplified assumption is adopted, setting the ratios between the three stiffness moduli— E_0^{ref}/E_{ur}^{ref} and $E_{ur}^{ref}/E_{50}^{ref}$ —equal to 3. This approach is commonly used when experimental data are incomplete. The reference oedometer tangent modulus is assumed to be $E_{oed}^{ref} = E_{50}^{ref}$. Moreover, this layer is not important in the considered problem.

Another important aspect of the analysis concerns the overconsolidation ratio (OCR) and earth pressure coefficient at rest (K_0) profiles. These profiles were generated assuming an equivalent pre-overburden pressure (POP) of 100 kPa, which aligns reasonably well with the OCR profile derived from Mayne's empirical relationship (Mayne et. al, 2023):

$$OCR = \left(\frac{0.192\left(q_t / p_a\right)^{0.22}}{\left(1-\sin\phi'\right)\left(\sigma_{v,0} / P_a\right)^{0.31}} \right)^{\left(\frac{1}{\sin\phi'-0.27}\right)} \tag{5}$$

The coefficient of earth pressure at rest, K_0, was then evaluated using the classical relationship:

$$K_0 = \left(1-\sin\phi'\right) OCR^{\sin\phi'} \tag{6}$$

with and upper bound limit of $K_0 < 1.5$ (after Mayne (Mayne et. al, 2023)).

The resulting OCR and K_0 profiles are shown in Fig.6.

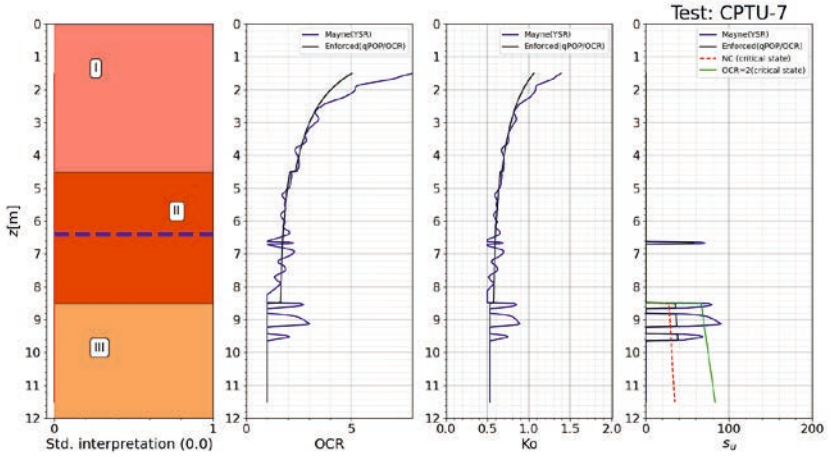

Fig. 6. Overconsolidation ratio () and coefficient of earth pressure at rest (K_0) profiles for the assumed equivalent pre-overburden pressure ($\mathrm{POP} = 100\mathrm{kPa}$ in Layer I, $80\ \mathrm{kPa}$ in Layer II and $OCR = 1$ is assumed in Layer III (own elaboration)

3.3. Summary of derived model parameters

Based on the analyses presented in the previous sections, the following initial guess of material parameters has been adopted for the three geotechnical layers. The strength and dilatancy parameters, along with the stiffness power exponents and Rowe's dilatancy law multiplier in the contractant domain (D), were derived from laboratory triaxial tests. In contrast, the stiffness moduli and the stress history parameter (POP) were calibrated using the results of the cross-hole and CPTU tests.

To avoid numerical instabilities caused by a large difference between friction angle ϕ' and dilatancy angle ψ the following limit has been assumed $\phi - \psi > 30°$.

Summary of all HS-Brick model parameters is given in Table 1.

https://doi.org/10.37705/TechTrans/e2025019

Table 1. List of HS-Brick model parameters (own elaboration)

Parameter	Unit	Layer I	Layer II	Layer III
E_0^{ref}	kPa	360000	200,000	280,000
γ	-	$4 \cdot 10^{-4}$	$2 \cdot 10^{-4}$	$2 \cdot 10^{-4}$
E_{ur}^{ref}	kPa	55560	55560	90000
ν	-	0.2	0.2	0.2
σ_{ref}	kPa	100	100	100
m	-	0.53	0.53	0.75
E_{50}^{ref}	kPa	19300	19300	30000
E_{oed}^{ref}	kPa	19300	19300	30000
ϕ'	°	34.4	34.4	32
ψ	°	4.4	4.4	2
c'	kPa	5	5	5
D	-	0.3	0.3	0.25
POP/OCR	kPa	100/-	80/-	-/1

4. Numerical FEM modeling of footing

The numerical FE model was developed using the ZSoil software v.2025 (ZSOIL, 2025), in which the HS-Brick constitutive model is implemented. To simplify the model setup, the soil layer above the foundation bottom was not discretized; instead, its effect was represented by equivalent distributed loads corresponding to the embedment depth of 0.899 m. To reproduce the complete stress history, the initial state considered in-situ conditions prior to excavation (by 1.5 m) and before the foundation construction. Subsequently, the overburden was removed, and the foundation was introduced. This stage was treated as the reference configuration for tracing the force–displacement response during the loading program.

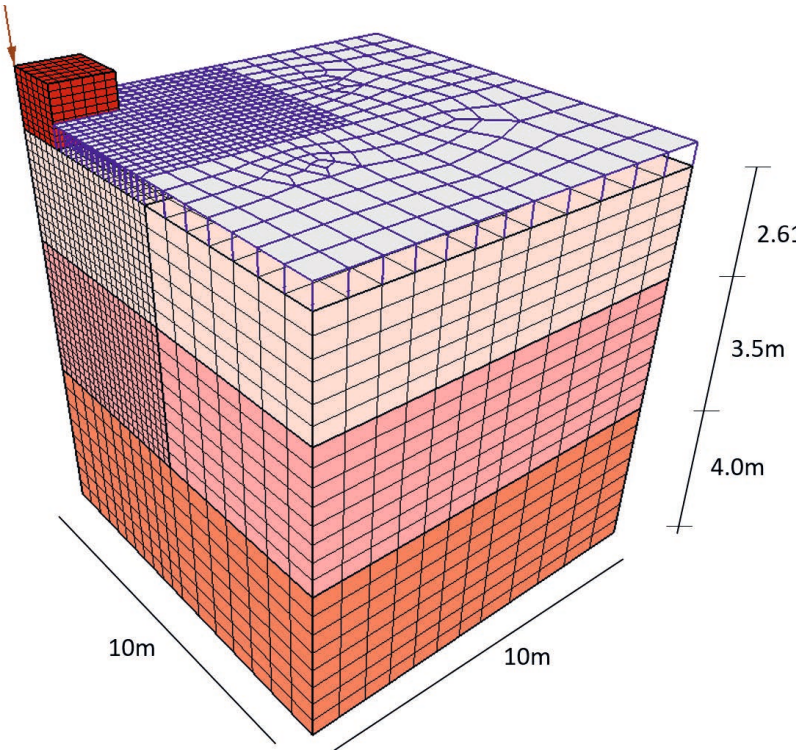

Fig. 7. FEM discretization and mesh geometry (own elaboration)

The FE mesh is presented in Fig. 7. Owing to geometric and loading symmetries, only one quarter of the model domain was analyzed, with 25 % of the total nodal load applied to the foundation. Seepage surface elements were introduced along the external model boundaries, where a fluid head boundary condition was applied, assuming the groundwater table at a depth of 4.01 m. The analysis was performed in an uncoupled manner, as consolidation effects were considered negligible.

Foundation is separated from the subsoil through the Coulomb's frictional interface characterized by friction angle $\phi_i = 20^\circ$.

5. Results of simulations

A comparison of the force–displacement diagrams obtained using the initial parameter set (Table 1) is presented in Fig. 8. The predicted settlements show very good agreement with the measured values, contradicting the conclusions reported in (Moussa, 2025). It can be observed that the average slopes of the unloading–reloading branches are nearly parallel to the measured ones, indicating that both the unloading–reloading and initial stiffness moduli are well reproduced. The initial mismatch results from an overly rapid degradation of the initial stiffness, governed by the parameter $\gamma_{0.7}$. Increasing this parameter to $\gamma_{0.7} = 6 \cdot 10^{-4}$improves the agreement. Qualitatively, such an increase in $\gamma_{0.7}$ may be expected in the case of aged soils.

An extended sensitivity analysis of the examined problem lies beyond the scope of this article and will be presented in a forthcoming paper covering the complete set of reported footings. In that study, the Kucherenko sensitivity indices will be evaluated for each specific branch of the force–settlement curve, and the optimal model parameters will be identified using metamodeling in combination with differential evolution algorithms.

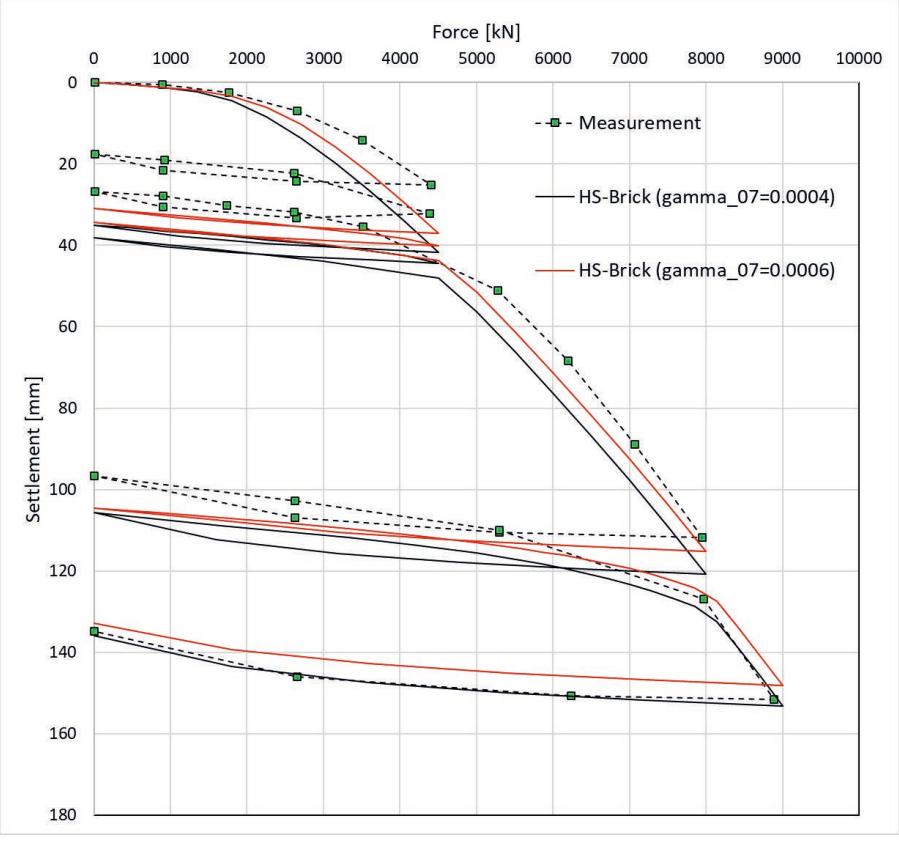

Fig. 8. Comparison of predicted and measured load-settlement diagrams (own elaboration)

https://doi.org/10.37705/TechTrans/e2025019

6. Conclusions

In this study, it has been demonstrated that the HS-Brick model, enhanced with extensions addressing the issue of unrealistically high undrained shear strength in dilatant soils and incorporating mean-stress-based stiffness barotropy, can reproduce triaxial test results with a high degree of accuracy.

It has also been shown that tests conducted over a wide range of confining stresses may preclude direct estimation of model parameters, as some samples are sheared under stress significantly below the preconsolidation level, while others lie within the normally consolidated range. In such cases, model parameters must be optimized using global search algorithms such as particle swarm optimization or differential evolution. However, these methods can be computationally expensive, even for relatively simple problems such as the triaxial test. To address this, a preliminary sensitivity study was performed, demonstrating that 100–200 optimized parameter samples can be generated using the Latin hypercube sampling method. This data can then be used to construct a robust metamodel that serves as a surrogate output generator, effectively replacing the finite element (FEM) solver. This methodology proved to be highly efficient.

In the second part of this study, a benchmark problem involving a spread footing founded on overconsolidated sandy soil in Texas was analyzed. The influence of soil aging was carefully examined, and potential sources of error in model parameter calibration were identified. Using the methodology proposed by Truty (Truty, 2024), all HS-Brick model parameters were derived while explicitly accounting for estimation uncertainties. The resulting parameter set produced very good agreement between the measured and predicted force–settlement relationships.

The proposed approach has proven to be both accurate and computationally efficient and can be readily applied to reliability-based geotechnical design in future engineering practice.

References

Andrus, R.D., Mohanan, N.P., Piratheepan, P., Ellis, B.S., & Holzer, T.L. (2017). Predicting shear wave velocity from cone penetration resistance. In *Proceedings of 4th International Conference on Earthquake Geotechnical Engineering*, June 25-28, Thessaloniki.

Benz, T. (2007). *Small-strain stiffness of soils and its numerical consequences*. Phd, Universitat Sttutgart.

Briaud, J.-L. & Gibbens, R. (1997). Large scale load test and data base of spread footings on sand. *Technical Report Publication No. FHWA RD-97-068*, Texas A&M University.

Briaud, J.-L. & Gibbens, R. (1999). Behavior of Five Large Spread Footings in Sand. *Journal of Geotechnical and Geoenvironmental Engineering. Journal of Geotechnical and Geoenvironmental Engineering 125*(9), https://doi.org/10.1061/(ASCE)1090-0241(1999)125:9(787)

Cudny, M. & Truty, A. (2020). Refinement of the hardening soil model within the small strain. *Acta Geotechnica 150*(8):0, 2031–2051

Lai, F., Tschuchnigg, F., Schweiger, H.F., Songyu Liu, Jim Shiau & Guojun Cai (2025). A numerical study of deep excavations adjacent to existing tunnels: integrating CPTU and SDMT to calibrate soil constitutive model. *Canadian Geotechnical Journal 62*, 1–23. https://doi.org/10.1139/cgj-2024-0203

Kawa, M., Puła, W., Truty, A. & Różański, A. (2025). *Probabilistic analysis of deflection of an anchored diaphragm wall for Hardening Soil model and nonlinear model of concrete. Proc. of the 9th International Symposium on Geotechnical Safety and Risk (ISGSR)*. Singapore: Research Publishing.

Kawa, M., Puła, W. & Truty, A. (2025). Probabilistic analysis of crack width and deflection of an anchored diaphragm wall installed in sand. *Archives of Civil and Mechanical Engineering 25*, 179. https://doi.org/10.1007/s43452-025-01230-6

Mayne, P.W., Cargill, E. & Greig, J. (2023). *The cone penetration test: better information better decisions*. A CPT Design Parameter Manual. ConTec.

Niemunis, A. & Cudny, M. Discussion on "Dynamic soil-structure interaction: A three-dimensional numerical approach and its application to the Lotung case study". Poor performance of the HSS model. Comput. Geotech. 98, 243–245 (2018).

ZSOIL User manual ZSoil v2025. Soil, Rock and Structural Mechanics in dry or partially saturated media. Geodev, Lausanne, Switzerland.

Moussa, A. (2025). Numerical modeling of scale load testing on spread footings in sandy soil: a comparative analysis of HSM and HYPO-Small models. *Journal of Engineering and Applied Science 72*(33). https://doi.org/10.1186/s44147-025-00602-2

Obrzud, R. & Truty, A. (2020). *The Hardening Soil Model. A practical guidebook*. Report 100701.

Robertson, P.K., & Cabal, K.L. (2022). *Guide to Cone Penetration Testing*. Signal Hill, CA.

Schanz, T. & Vermeer, P. (1998). On the stiffness of sands. In Jardine R., Davies M., Hight, D., Smith A., and Stallebras S. (eds.) *Pre-failure deformation behaviour of geomaterials* (pp. 383–387). London: Thomas Telford.

Schanz, T., Vermeer, P. & Bonier, P. (eds.) (1999). *Formulation and verification of the Hardening Soil model. Beyond 2000 in Computational Geotechnics*. Rotterdam: Balkema.

Truty, A. (2024). Estimating Hardening Soil-Brick model parameters for sands based on CPTU tests and laboratory experimental evidence. *Scientific Reports 14*, 15102. https://doi.org/10.1038/s41598-024-65789-5

Truty, A. & Obrzud, R. (2015). Improved formulation of the Hardening Soil model in the context of modeling the undrained behavior of cohesive soils. *Studia Geotechnica et Mechanica* 37(2), https://doi.org/10.1515/sgem-2015-0022

Wichtmann, T., Kimmig, I. & Triantafyllidis, T. (2017). On correlations between "dynamic" (small-strain) and "static" (large-strain) stiffness moduli – an experimental investigation on 19 sands and gravels. *Soil Dynamics and Earthquake Engineering 98*(4), 72–83.

Wichtmann, T. & Triantafyllidis, T. (2009). Influence of the Grain-Size Distribution Curve of Quartz Sand on the Small Strain Shear Modulus . *Journal of Geotechnical and Geoenvironmental Engineering. ASCE 135*(10), 1404–1418.